



ON THE MSD ASSESSMENT OF REAL AIRCRAFT FUSELAGE PANELS

Garcia, Abilio Neves & Mello Jr., Alberto Walter da Silva

Institute of Aeronautics and Space
Praça Marechal Eduardo Gomes, 50.
Campus do CTA
IAE/ASA
12228 904 – São José dos Campos – SP – Brazil
Tel.: +55(0)12 39473424 Fax: +55(0)12 39473325
E-mail: abilio.garcia@iae.cta.br

ABSTRACT

This paper presents the current investigation stage of Multiple Site Damage (MSD) assessment by the Structural Integrity Group from the Brazilian Air Force (FAB) located at the Aerospace Technical Center (CTA), Brazil.

Among all aeronautical structures prone to develop MSD, riveted lap joints in the fuselage have been identified as being the most susceptible. Recent recommendations by regulators to avoid MSD threat stipulate an Inspection Starting Point (ISP) and a Structural Modification Point (SMP) in the life of aircraft. These points can be defined with the help of MSD analysis and the capability to accurately calculate service life to MSD onset becomes of considerable importance. To investigate this failure mode, a probabilistic model for MSD assessment considering both fatigue crack initiation and crack propagation as random variables is used. Previous publications from the author demonstrated the effectiveness of this model by providing good agreement with experimental work on fatigue of riveted lap-splice joints. The literature widely reports the use simple fatigue test specimens, manufactured using aircraft standards (material, rivets and assembly techniques), to derive S-N fatigue initiation data for MSD assessment models. A direct consequence of this practice is that MSD models can be actually describing MSD behaviour of flat lap joint panels in laboratory environment and not real aircraft structures.

This work presents the MSD assessment results compared to teardown data obtained from in-service fuselage panels of aging aircraft. Evidences from in-service MSD detection strongly indicate that S-N input data obtained from good quality riveted flat lap joint test specimens can not be used for MSD assessment of real aircraft pressurized fuselage panels. These evidences are also supported by an in-house probabilistic fatigue crack initiation analysis using S-N data from good quality riveted lap joints for the in-service geometrical configuration analysed. For such reasons, the MSD assessment presented in this work was performed with open hole quality S-N fatigue crack initiation data. The results indicated that the mean cumulative probabilities for fatigue crack initiation, crack detection and failure were rationally conservative, with differences in the order of 20 %, when compared to the corresponding distributions for the in-service findings.

1. INTRODUCTION

Large passenger aircraft when kept in service for an extended period of time suffer from the development of a range of damage processes associated with ageing aircraft. These can take the form of corrosion, together with various forms of fatigue failure. Multiple Site Damage (MSD) is one of the major threats to airworthiness of such ageing aircraft. MSD is the simultaneous development of fatigue cracks at an array of similar structural details. MSD has been most



apparent in fuselage lap joint structures, and can result in unexpected catastrophic failure of aircraft, as it is difficult to detect. Recent recommendations by regulators to avoid this MSD threat [1] stipulate an Inspection Starting Point (ISP) and a Structural Modification Point (SMP) in the service life of aircraft. These points can be defined in terms of MSD analysis results, test results and/or by service experience. The intention is that the aircraft shall not be operated while there is a significant probability that MSD is present. Capability to accurately calculate service life to MSD onset becomes of considerable importance.

Previous workers have approached this problem by considering the probabilistic nature of MSD occurrence, and have employed Monte Carlo techniques to simulate the stochastic nature of fatigue crack initiation at fastener holes and/or subsequent crack propagation, and therefore calculate the distribution of lives to MSD onset, link-up and ultimate failure.

The crack initiation stage is commonly addressed by applying Monte Carlo simulation to lognormal or Weibull distributions of lives to achieve a specified crack size a_0 [1]. The following crack propagation stage is simulated either deterministically or probabilistically. There are particular difficulties in calculation of stress intensities for crack growth in MSD crack configurations because the β correction term will change for every different crack configuration simulated. Therefore the technique used for stress intensity calculation must be accurate and economical of computer time if it is to be used in a repeated simulation such as the Monte Carlo. In previous work, finite elements [2], alternating finite elements [3], boundary elements [4], dual boundary elements [5] and compounding method [6] have all been used to calculate stress intensities of MSD cracks.

Over the past 15 years, there have been several Monte Carlo simulations of the MSD life calculation problem. These have differed greatly in their built-in assumptions, approximations and their calculation techniques. In consequence the predicted life distributions have also varied from simulation to simulation, as has the level of agreement with experimental data. The Dual Boundary Element (DBE) technique for calculation of stress intensities in MSD situations has advantages in accuracy over other numerical techniques [7]. Previous MSD simulations using DBE have used deterministic crack growth together with open hole geometries in their analysis [5]. In this work the DBE method has been applied to a row of pin loaded holes to perform probabilistic crack growth simulation of MSD using the Monte Carlo approach.

2. A METHODOLOGY FOR MULTIPLE SITE DAMAGE ASSESSMENT

Details of the MSD assessment model employed in this work is presented in the next sections. The modelling procedures are separated into different stages: fatigue crack initiation, deterministic crack propagation and probabilistic crack propagation.

2.1. Fatigue Crack Initiation

To represent the fatigue crack initiation life ' N_0 ', a lognormal distribution of lives to achieve a crack size of ' a_0 ' is employed. Considering the external rows of a lap joint, it is assumed that each pin-loaded hole has two fatigue critical locations (FCL) at 3 and 9 o'clock positions of the hole border. For each FCL, the normal distribution ' $\log(N_0)$ ' is defined by the mean S-N fatigue life ' μ ', the standard deviation ' σ ' and the standard normal distribution ' α ' given by,

$$\log(N_0) = \mu + \alpha \cdot \sigma \quad (1)$$

When a random value of ' α ' is generated by Monte Carlo simulation, one initial damage scenario is created by attributing each FCL a different initial fatigue life given by equation 1.

2.2. Deterministic Crack Propagation

The DBEM formulation utilized here for stress intensity calculation was developed by Salgado [7, 8], and it has been incorporated in the DTD code [9] for crack growth life calculation used in this work. Crack tips emanating from pin loaded fastener holes are subjected to mixed mode stress fields, and the DBE program calculates both K_I and K_{II} components. A mixed mode stress intensity range ΔK_{eff} was calculated using the expression [10]

$$\Delta K_{eff} = \sqrt{\Delta K_I^2 + 2\Delta K_{II}^2} \quad (2)$$

The Paris equation is used to calculate the crack growth rate (da/dN), given as a function of the effective stress intensity factor (ΔK_{eff}),

$$\frac{da}{dN} = C(\Delta K_{eff})^n \quad (3)$$

Material constants C and n values are obtained from Salgado [9]. Crack growth lives are then calculated in the usual way using equation 3, with a starting crack length a_0 in the macro crack size range. As cracks grow, the Swift [11] criterion is used to define link-up. After link-up with an uncracked hole, continuing damage [12] is assumed (an initiated crack of length 0.127 mm is assumed to start from the opposite hole border to where link-up took place). Final failure occurs when residual strength becomes inadequate on either material fracture toughness or net-section yield criteria.

2.3. Probabilistic Crack Propagation

Possibly the first work to demonstrate the probabilistic nature of crack growth was presented by Virkler [13] by means of sixty eight replicate constant amplitude crack propagation tests conducted on 2024-T3 aluminium alloy (Figure 1). Virkler verified that fatigue crack propagation process presents a scatter, and so does the crack growth rate (Figure 2).

From the results presented in Figure 1, Virkler observed that if a ‘test started out slow it tended to remain slow for most of the test’. From Figure 1, it can also be stated the opposite situation: tests that start out fast tend to remain fast.

In order to represent the probabilistic nature of fatigue crack growth in this work, the Xing [14] formulation will be used to couple Monte Carlo simulation to the deterministic numerical technique for crack propagation presented in section 2.2. Considering the modified Paris equation 3, reproduced here as follows,

$$\frac{da}{dN} = C(\Delta K_{eff})^n \quad (4)$$

Taking the logarithm on both sides of equation 4 it follows,

$$\log \frac{da}{dN} = \log C + n \log(\Delta K_{eff}) \quad (5)$$

To represent the stochastic nature of crack propagation, a normally distributed variable $Z \sim N(0, \sigma_z^2)$ is added to the logarithm of the fatigue crack growth equation 5,

$$\log \frac{da}{dN} = \log C + n \log(\Delta K_{eff}) + Z \quad (6)$$

Considering the properties of the standard normal distribution $[N(0,1)]$, the probability that a measurement will fall in a range $Z \leq Z_p$ is given by $P(Z \leq Z_p) = p$, and Z_p can be written as,

$$Z_p = \alpha_p \sigma_z \quad (7)$$

When the probability ‘ p ’ is given, α_p can be obtained from the standard normal distribution. For example, when $p = 50\%$, $\alpha_p = 0$, leading $Z_p = 0$ in equation 7, and equation 6 becomes equation 5 which becomes equation 4 which is the deterministic average fatigue crack growth rate. The probabilistic crack growth rate, represented by equation 6, can be simplified if the value of ‘ n ’ is assumed as a mean constant value and the probabilistic character of crack growth is attributed to ‘ C ’, assumed as a lognormal distribution. The assumption of considering ‘ n ’ constant and varying ‘ C ’ as a lognormal distribution is enough to adequately describe the crack propagation rate and its statistical feature [15, 16]; and it has been widely employed by the MSD models from the literature when probabilistic crack growth is considered. Therefore, equations 6 and 7 can be re-arranged as,

$$\log \left(\frac{da}{dN} \right)_p = \log C_p + n \log(\Delta K_{eff}) \quad (8)$$

Where $\log C_p = \log C + \alpha_p \sigma_z$ is now a random variable normally distributed with mean $\log C$ and variance σ_z^2 . Equation 8 can be re-written as,

$$\frac{da}{dN} = [C \exp(\ln 10 \cdot \alpha_p \cdot \sigma_z)] (\Delta K_{eff})^n = \bar{C} (\Delta K_{eff})^n \quad (9)$$

At the original work from Xing [14], equation 9 is derived from equation 4 as presented in this section, but taking the natural logarithm both sides from equation 4 which leads equation 9 to be written as,

$$\frac{da}{dN} = [C \exp(\alpha_p \cdot \sigma_z)] (\Delta K_{eff})^n = \bar{C} (\Delta K_{eff})^n \quad (10)$$

The difference between equations 9 and 10 is because in the former the value of σ_z is given in log-scale and in the latter it is given in natural-log-scale. As values of σ_z are more commonly found in the literature in log-scale, in this work equation 9 is adopted for probabilistic crack growth analysis.

For a given value of α_p , the number of cycles N_f to grow a crack from an initial crack size 'a₀' up to a crack size 'a_f' is obtained from direct integration of equation 9,

$$N_f = \frac{1}{C} \int_{a_0}^{a_f} \frac{da}{(\Delta K_{eff})^n} \quad (11)$$

Based on Virkler findings described in the beginning of this section, it is assumed in this work that each initial damage scenario generated by Monte Carlo simulation (section 2.1) has a unique α_p value in equation 11, i.e., in practice each damage scenario is assigned a random ' \bar{C} ' value so that deterministic crack propagation can now be performed.

The effect of considering 'n' constant and 'C' varying as a lognormal distribution is illustrated in Figure 3; where it can be seen that parallel crack growth rate curves are created to describe the scatter from Figure 2.

2.4. Methodology Comparison to Experimental Work (Riveted Flat Panel)

The lap joint geometry which is analysed is shown in Figure 4 and consists of 3 rows of 9 pin loaded holes. It is subjected to a uniform remote alternating tensile stress with maximum stress of 100 MPa and R = 0.1. The sheet is 1.6 mm thick and is of clad 2024 T3. The rivet diameter (ϕ) is 4 mm, and the pitch distance (p), the inter row spacing (s) and the edge distance (e) are all equal to 20 mm. Material properties are $\sigma_{UTS} = 448$ MPa, $\sigma_{YS} = 331$ MPa and $K_{IC} = 32$ MPa m^{1/2}. Material constants for deterministic crack growth C and n values (equation 3) are C =

6.09E-11 and $n = 2.6$, obtained from Salgado [9]; and $\sigma_z[\log] = 0.043$ has been assumed, following Proppe [3], for probabilistic crack growth (equation 11). It has to be highlighted that the value of K_{1C} from the DTD code (32 MPa m^{1/2}) for Al2024-T3 is set automatically for plane strain condition showing that the author [9] of the code chose a conservative approach when calculating critical crack size values via the fracture toughness failure criterion. The S-N fatigue curve properties used for the riveted holes is from Santgerma [2], and the values for ' $\mu[\log]$ ' and ' $\sigma[\log]$ ' are, respectively, 5.6370 and 0.20 for an initial crack size a_0 of 1.5 mm. For each damage scenario generated by Monte Carlo simulations, the crack growth life is, firstly, calculated in a deterministic way, as described in section 2.2, and, secondly, the probabilistic treatment, as described in section 2.3, is applied.

The results of 400 Monte Carlo simulations are presented in Figure 5, together with 6 points from the test results of Foulquier [17]. The position of the limits of the confidence regions [18] have been corrected according to Arnold [19], so that a finite number of random simulations can produce the same confidence region size as an infinite number of simulations.

As found in other published simulations, for instance Santgerma [2], Proppe [3] and Kebir [5], Figure 5 shows that lives to failure are dominated by crack initiation, with initiation life occupying between 3-15 times the total propagation life. Total initiation life varies from 5.5×10^4 to 3.7×10^5 cycles, whereas propagation lives are between 1.5×10^4 to 7×10^4 . Five of the six experimental points fall on or outside the 95% probability boundary line for the simulations, suggesting that real failure processes have considerably greater variability than the simulations. The mean propagation life of the experimental data is approximately the same as that of the simulations, but the spread of the 6 experimental propagation lives is as large as that of the entire 400 simulations. The spread of predicted lives encloses the range of scatter of the experimental lives for both initiation and propagation stages. However, there are only 6 experimental points; even for the 99.7 % confidence region there is one experimental point standing outside. It is likely that were 400 experiments to be performed, the observed scatter could be significantly greater than the current data set.

In order to derive [1] the Inspection Starting Point (ISP) and the Structural Modification Point (SMP), used to establish the monitoring period, the mean fatigue life to failure (N_f, mean) must be determined. From Figure 5, the value of N_f, mean is given by $N_f, \text{mean} = N_{\text{initiation}, \text{mean}} + N_{\text{propagation}, \text{mean}} = 222,000$ cycles. The ISP and the SMP are calculated by dividing N_f, mean by typical factors of 3 and 2 respectively [1]. For these numbers and for the joint analysed in this work (Figure 4), the ISP and the SMP values are respectively, 74,000 cycles and 111,000 cycles. Repeat inspection intervals (I_{WFD}) are established based on time from a

detectable crack size initiation up to the SMP, divided by a factor (F_{WFD}). Considering the chosen initial crack size value of 1.5 mm as the detectable crack length, the total Inspection Period (IP) is defined as the cycles between the ISP and the SMP, i.e., equal to 37,000 cycles. From the 99.7 % confidence limits of Figure 5, it can be noticed that the smallest time to crack propagation ($TTCP_{MIN}$) up to failure is 12,000 cycles. According to traditional damage tolerance analysis, if $TTCP_{MIN}$ is divided by a safety factor of 2 it will lead to an inspection period of 6,000 cycles. Dividing the IP by 6,000cycles, a factor $F_{WFD} = 6.2$ is obtained and, consequently, a factor of 7 is more likely to be employed. Therefore, the repeat inspection intervals can be defined as $I_{WFD} = IP/F_{WFD} = 5,285$ cycles which can be approximated to $I_{WFD} = 5,200$ cycles. However the approximations and assumptions inherent in the current model, some of which are discussed above, the results suggest that we cannot yet regard the factors used in the derivations as fixed. It may be that distributions of real test data gathered on large numbers of aircraft would have distributions for which use of the above factors would not result in an acceptably low probability of occurrence of MSD.

3. MSD Assessment Comparison to Teardown Inspections from In-Service Data

In section 3.2, an MSD assessment analysis is presented to compare its output to teardown data obtained from in-service fuselage panels of aging aircraft published by Steadman [20]. The lap joint geometrical configuration analysed is presented in Figure 6 and it is from a Boeing 727 aircraft [20]. The fuselage skin is of aluminium 2024-T3, the outer and inner skins thicknesses are, respectively, 1.6 mm and 1.0 mm; and they are connected by 3 rows of NAS1097D6 aluminium rivets of diameter 4.76 mm, row spacing of 22.9 mm and pitch distance between rivets of 28.6 mm. The frame spacing is of 508 mm and 17 rivet holes are present within one frame bay, excluding the ones from the frames. The lap joint configuration is subjected to a nominal hoop stress of 103.4 MPa at fuselage skin mid-frame bay due to pressurization.

3.1. Why open hole / loose fit loaded hole S-N data for fatigue crack initiation?

To analyse the fuselage panel configuration presented in Figure 6, it was assumed an open-hole quality S-N fatigue data for fatigue crack initiation. As lap joint configurations for real fuselage panels are riveted, this assumption must be explained.

From some MSD models presented in the literature, for example Schmidt [21], it is a common practice to use flat straps of riveted specimens, manufactured using aircraft standards (material, rivets and assembly techniques), to derive S-N fatigue data for MSD assessment comparison to fatigue tests of flat fuselage panel sections subjected to multiple cracking. Of course, these comparisons are valid to demonstrate the effectiveness of the methodologies since the models output represents what is intended for comparison. A direct consequence of this issue is that

MSD models can be describing the MSD behaviour of flat sections of riveted panels in laboratory environment, but not real aircraft structures [22].

Real aircraft fuselage lap joints are subjected to bi-axial loads such as circumferential and axial stresses caused by pressurization, bending and torsion caused by aerodynamic loads, inertia loads and landing, not to mention environmental issues such as corrosion. In his work, Okada [23] compares the fatigue lives for initiation of 1 mm cracks from flat panel specimens and one-third scale-models of a B-737 fuselage structure subjected to pressurization and bending loads. If the fatigue life for crack initiation obtained from the scale-model specimens is divided by the corresponding value from flat panel specimens, a mean coefficient of 0.42 is obtained. This coefficient means that the fatigue life for crack initiation is reduced by 58 % when curved panel test specimens are considered. It has to be highlighted that the mean coefficient of 0.42, derived by the author from Okada [23] experimental work, was calculated based on two flat lap joint and two scale-model fatigue test specimens; which cannot represent the statistical dispersion inherent to a wider number of fatigue tests. But, certainly, Okada [23] experiments give a clear indication that there are significant differences from both fatigue test specimens as a source for input data for Monte Carlo simulations.

Another indication that pristine and good quality riveted flat lap joint test specimens are possibly not indicated to generate S-N fatigue data for MSD assessment of real fuselage panels comes from Wanhill [24], Bakuckas [25] and Steadman [20]. Wanhill [24] presents the service histories of pressurized fuselage lap splices from five different in-service aircraft types where MSD cracking was detected. By the time MSD was identified, the number of flights varied from 34,470 to 75,158. From Bakuckas [25] it is also reported MSD occurrence, detected by current methods for field inspections, from a retired Boeing 727 containing 59,497 flight cycles. Steadman [20] findings were that MSD initiation was reported even before 20 % (12,000 flight cycles) of the Design Service Goal (DSG). These numbers are showing that MSD occurrence, from in-service or retired fuselage panels, happens in a range of $1E+4$ to $1E+5$ flight cycles; while fatigue lives to crack initiation from S-N tests of pristine and good quality strap joints are commonly reported to be higher than $1E+5$ cycles at typical loads around 100 MPa and R ratios ranging from 0 to 0.1 [26].

Another complicating factor, when assessing real fuselage panels for MSD behaviour via fatigue data from flat lap joint specimens, is corrosion. Corrosion occurrence has been reported from retired and in-service aircraft fuselage joints [27]. Concerning S-N fatigue data itself, a comparison between fatigue tests from pristine and corroded flat lap joint samples showed that corrosion can easily degrade the fatigue life for visible crack initiation by 40 % [28]; and,



therefore, pristine test specimens seem not to be adequate to approach real aircraft fuselage panels if corrosion is considered.

For the arguments presented in the previous paragraphs, the applicability of fatigue crack initiation data obtained from pristine and good quality riveted flat lap joint test specimens for MSD assessment of real aircraft fuselage panels is questioned by the author.

From the literature, a positive indication that flat riveted lap joint test specimens could be used for comparison to full-scale fatigue tests (which mostly resembles in-service fuselage panels) comes from Horst [29]. From his MSD simulations, Horst could predict a full-scale fatigue test result at the border of his 99.7 % confidence region where the smallest fatigue lives were obtained from the simulations. It has to be highlighted that Horst employed a poor quality deep countersunk riveted joint to force early fatigue crack initiation because, according to his arguments, good quality riveted samples would be inadequate for comparison purposes with the full-scale test due to the high fatigue lives obtained from those samples. The result from the full-scale fatigue test [29] presented a detectable crack with fatigue life around 80,000 pressurization cycles and, as observed from in-service fuselage panels, a fatigue life in the range of $1E+4$ to $1E+5$ cycles.

As an exercise, and considering the lap joint configuration from Figure 6, S-N fatigue data obtained from good quality riveted flat lap joint test specimens can be found in Swift [30]; and calculating the mean time to crack initiation it is obtained, approximately, $1E+6$ cycles. If a typical standard deviation value of 0.15 in log (cycles) is assumed for fatigue crack initiation of Al 2024-T3 riveted panels [31], the results from Monte Carlo simulations will give a mean time to crack initiation of the lead crack equal to 536,250 cycles; with the smallest and biggest lives equal to, respectively, 266,088 and 835,761 cycles. From this exercise, it is quite clear that MSD assessment of real aircraft fuselage panels, when performed with input S-N fatigue life data from good quality riveted flat lap joint samples, is destined to a terrible non-conservatism. This statement is easily verified if lives to MSD occurrence from aging aircraft pressurized fuselage panels (34,470 to 75,158 cycles [24]; 59,497 cycles [25]; 12,000 cycles [20]) are compared to the fatigue crack initiation lives generated by the Monte Carlo simulations from the present exercise (266,088 to 835,761 cycles).

Therefore, for the reasons presented so far, the author decided to assume open hole quality S-N fatigue data input for the fatigue crack initiation part of the MSD assessment model.

3.2. MSD Assessment Comparison to Teardown Inspections from In-Service Data

According to Steadman [20], MSD was detected at the inner fuselage skin at the rivet lower row (Figure 6) and cracks nucleated basically at holes from the centre of the bay. The DBE model

idealized to analyse the inner skin of the lap joint configuration from Figure 6 is presented in Figure 7.

The DBE model from Figure 7 consists of one rectangular sheet of aluminium 2024-T3; 1000 mm long and 314.4 mm wide; discretized by 182 boundary elements and 364 nodes; with a central row of 11 pin-loaded holes; lateral constraint (D_x) in the x direction to simulate a wider joint, top and bottom constraint (D_x) in the x direction and lateral constraint (D_y) in the y direction where no displacements are expected due to symmetry; gross stress (T_y) applied in the top of the model and bypass stress (T_y) applied in the bottom of the model. The hole diameter, pitch distance between holes and sheet thickness are the same as illustrated in Figure 6 for the inner skin.

The bypass stress ($\sigma_{bp} = 66.7$ MPa) and the bearing stress ($\sigma_{br} = 220.2$ MPa) for the DBE model from Figure 7 was obtained considering a gross stress $\sigma_{gross} = 103.4$ MPa applied to a strap lap joint subjected to load equilibrium, but with width of 28.6 mm (one pitch distance) and all remaining dimensions as from Figure 6 inner skin. All the 11 holes from Figure 7 have the same pin-loading (uniform pin-loading) and they represent the inner skin lower row of rivet holes present in the central part of the fuselage bay from Figure 6.

Figure 8 presents S-N fatigue data [30] for cycles to failure of a loose fit/open hole strap specimens of aluminium 2024-T3, which is adopted in this section for the fatigue crack initiation part of the MSD assessment model. The material and dimensions of the strap specimen used to generate the S-N data from Figure 8 are the same as for the inner skin from Figure 6, but the specimen width is of 31.8 mm.

As it can be seen, Figure 8 presents the S-N data as a function of the gross stress (σ_{gross}) and the stress ratio $\sigma_{br} / \sigma_{gross}$. For the calculated loading conditions used in this section $\sigma_{gross} = 103.4$ MPa (15 ksi) and $\sigma_{br} / \sigma_{gross} = 2.13$, the fatigue life to failure of the strap specimen is equal to 42,000 cycles. The value of 42,000 cycles to failure has to be normalized to achieve a fatigue life corresponding to an initial crack size to serve as input variable for the crack initiation part of the MSD assessment model. In his work Steadman [20] presents a cumulative distribution function for fatigue crack initiation corresponding to an initial crack size of 1.27 mm (0.05 inches), which is adopted in this section.

To normalize the 42,000 cycles to failure to a fatigue life corresponding to an initial crack size of 1.27 mm; a DBE strap lap joint model was built, but to represent the strap specimen configuration at the top right from Figure 8. The loading condition was a maximum tensile stress of 103.4 MPa and $R = 0$. The number of cycles to propagate an initial crack size of 1.27

mm up to failure from the DBE strap model was 6,300 cycles, which subtracted from 42,000 cycles to failure gives a mean time to crack initiation of 35,700 cycles or 4.5527 in log (cycles). With the mean time to crack initiation defined, the corresponding standard deviation value has to be established. As from Figure 8 no information about scatter is provided, it is assumed a standard deviation of 0.15 (log-scale) to be a typical value for fatigue testing of aluminium alloy 2024 components under constant amplitude loading [31].

Figure 9 presents cumulative probability distributions from the detailed results of teardown inspections on 24 fuselage bays calculated by Steadman [20]. The x-axis presents life in terms of percent of DSG (Design Service Goal), where 100 % DSG is equal to 60,000 flight cycles. The y-axis presents the cumulative probabilities from 0 to 1 (0 to 100 %). In the legends, 'Initiation' is the cumulative distribution for initiation of fatigue cracks with a crack length of 1.27 mm; 'Detectable' is the cumulative distribution to detect a crack length of 5.1 mm with 66 % probability; and 'Failure' is the cumulative distribution for the link-up of adjacent MSD cracks.

In this section failure is defined as the first crack link-up, i.e., crack propagation is performed considering an initial crack size of 1.27 mm up to the link-up of a crack with another crack to compare with the results from Figure 9.

To check for crack propagation obtained with the DBE model from Figure 7; Figure 10 presents fleet crack growth data [32] for Boeing 737 and 727 aircraft together with 'This work' deterministic crack propagation data. From Figure 10, Jones [32] highlights one crack growth region between the horizontal lines that cross the 4 and 11 mm crack length axis. It can be seen that, within the region defined, the crack propagation time ranges from, approximately, 16,000 to 45,000 flight cycles for several B-737 and B-727 aircraft. The crack growth data plotted as 'This work' indicates a number of, approximately, 26,000 cycles to grow a single crack from 4 up to 11 mm; which demonstrates that the number of cycles obtained for 'This work' is within the range of the data measured from real aircraft fuselage panels.

The result of Monte Carlo simulations regarding 11 central holes for the idealized inner skin lower row of rivets from Figure 6 is presented in Figure 11. It can be seen that lives to failure (initiation + propagation lives) are dominated by crack propagation, with mean initiation life equal to 18,655 cycles (31.1 % DSG) and the mean propagation life equal to 23,890 cycles (39.8 % DSG), i.e., the propagation phase represents 56.2 % of the mean failure process (18,655 + 23,890 cycles = 42,545 cycles = 70.9 % DSG). Total initiation life varies from 9,536 to 28,780 cycles, whereas propagation lives are between 13,614 to 43,007 cycles.

Figure 12 shows the cumulative probability distribution comparison for crack initiation from the results presented in Figures 11 (Monte Carlo simulations) and 9 (teardown inspection data). The

x-axis shows life as a function of percentage of DSG and the y-axis the corresponding cumulative probabilities from 0 to 1 (0 to 100%). In the legends, 'Initiation' refers to the teardown data (Figure 9) while 'Initiation MC' to the Monte Carlo simulations (Figure 11).

From Figure 12, the 0.5 cumulative probabilities for initiation of fatigue cracks from the teardown data and from Monte Carlo simulations are, respectively, 36.9 % DSG (22,140 cycles) and 31.1 % DSG (18,665 cycles); with the Monte Carlo simulation results being 15.7 % smaller than the teardown inspection results.

Figure 13 shows the cumulative probability distribution comparison for crack detection. The results for Monte Carlo simulation from Figure 13 were obtained from the results presented in Figure 12 (initiation of fatigue cracks) but adding the number of cycles to grow the corresponding lead cracks probabilistically from 1.27 mm to 5.1 mm (detectable crack length considered in Figure 9).

From Figure 13, the x-axis shows life as a function of percentage of DSG and the y-axis the corresponding cumulative probabilities from 0 to 1 (0 to 100%). In the legends, 'Detectable' refers to the teardown data (Figure 9) while 'Detectable MC' to the Monte Carlo simulation results.

From Figure 13, the 0.5 cumulative probabilities for detection of fatigue cracks from the teardown data and from Monte Carlo simulations are, respectively, 68 % DSG (40,800 cycles) and 52.3 % DSG (31,380 cycles); with the Monte Carlo simulation results being 23.1 % smaller than the teardown inspection results.

Figure 14 shows the cumulative probability distribution comparison for failure, defined as first crack link-up, from the results presented in Figure 11 (Monte Carlo simulation) and Figure 9 (teardown inspection data). The x-axis shows life as a function of percentage of DSG and the y-axis the corresponding cumulative probabilities from 0 to 1 (0 to 100%). In the legends, 'Failure' refers to the teardown data (Figure 9) while 'Failure MC' to the Monte Carlo simulations (Figure 11).

From Figure 14, the 0.5 cumulative probabilities for failure from the teardown data and from Monte Carlo simulations are, respectively, 91.5 % DSG (54,900 cycles) and 70.9 % DSG (42,540 cycles); with the Monte Carlo simulation results being 22.5 % smaller than the teardown inspection results. With the mean number of cycles to failure established by Monte Carlo simulation, the ISP and the SMP are calculated as, respectively, 14,180 cycles (23.6 % DSG) and 23,270 cycles (35.5 % DSG); considering, respectively, factors 3 and 2 as recommended in reference [1]. The ISP and the SMP values for the Monte Carlo simulations from Figure 11 are 22.5 % smaller than the same values from the teardown data.

From Figure 12, it can be seen that the cumulative probabilities for fatigue crack initiation of the lead crack from the simulations is surprisingly close to the one from in-service data, more noticeably for low probabilities of occurrence. It can also be noted that the inclination of the distribution from the simulations is smaller than the one from in-service data, indicating that in reality a bigger standard deviation value should be used. If the mean times to crack initiation from the distributions are compared, then it can be seen that the value from the simulations is 15.7 % smaller than the one from in-service data. This result demonstrates that the use of open hole S-N data for fatigue crack initiation is rationally conservative, and for the case of the lap joint from Figure 6 can be applied.

From Figure 13, it can be seen that the differences between the cumulative distributions for detectable cracks are enlarged when compared to the results from Figure 12. Considering the mean time for detectable cracks (50 % probability), the Monte Carlo simulation result is 23.1 % smaller than the in-service ones. It has to be highlighted that the Monte Carlo simulation results from Figure 13 were obtained from the results presented in Figure 12 (initiation of fatigue cracks) but adding the number of cycles to grow the corresponding lead cracks probabilistically from 1.27 mm to 5.1 mm (detectable crack length considered by Steadman [20]). This procedure needs some extra refinement, since the scatter for the detectable crack distribution was simply attributed to the scatter inherent to the crack growth process but the crack detection itself presents a scatter inherent to the inspection process; and if this scatter is added to the one from the simulations the inclination of the present cumulative distribution is expected to increase. If only the crack propagation process is considered, then the enlargement of distance between both distributions from Figure 13, when compared to Figure 12, can be attributed to conservatism in the whole crack propagation calculations performed with the model from Figure 7.

From Figure 14 it can be seen that the cumulative probabilities of failure from the simulations and in-service data are enlarged when compared to Figure 12. The mean time for failure from the simulations is 22.5 % smaller than the in-service one. As for the case of Figure 13, this difference can also be attributed to conservatism in the whole crack propagation calculations performed with the model from Figure 7, but other reasons apply as well. From Figure 10, it can be seen that, although the crack propagation analysis from the simulations are comparable to in-service data [32], crack propagation times ranged from approximately 16,000 to 45,000 flight cycles for Boeing 727 and 737 aircraft; while the same value given by the model from Figure 10 was 26,000 cycles. These differences seem not to be connected, so lonely, to the scatter inherent to the crack growth process. It is possible that 'flight cycles' from Figure 10 do not necessarily mean full pressurization cycles, and this issue depends on the service history of each aircraft.

From the point of view of the AAWG recommendations [1], the basic purpose of MSD models is to establish both the ISP and SMP points, from the 50 % cumulative probabilities of failure (Figure 14), to define a monitoring period in order to prevent MSD threat. If the ISP and SMP points are considered, the calculated values from the analysis are, respectively, 14,180 cycles (23.6 % DSG) and 23,270 cycles (35.5 % DSG); while the same values calculated from the in-service data are, respectively, 18,300 cycles (33.3 % DSG) and 27,480 cycles (45.8 % DSG). These results indicate that the ISP and the SMP points established from the simulations are 22.5 % smaller than the ones from in-service data. From an engineering point of view, this difference is not small; but it is far from being unacceptably conservative considering that real MSD occurrence from aging aircraft pressurized fuselage panels is being assessed.

Returning to the points of ISP and SMP, established from both the in-service data and the simulations, these points define the monitoring period which is 'the period of time when special inspections of the fleet are initiated due to an increased risk of MSD' [1]; and the monitoring period ends when the SMP is reached. The SMP point, also called the 'point of WFD' (widespread fatigue damage) [1], is the point where 'no airplane may be operated without modification or part replacement' [1] or 'the point beyond which the airplane may not be operated without further evaluation' [1]; and at the SMP point, failure due to MSD should not represent a threat to structural safety due to high probabilities of occurrence. The reason for reminding the monitoring period and the SMP concepts is to verify whether these parameters (established by the simulations) are well suited to its definitions or not when compared to the in-service data; and to perform this verification the results from Figure 14 are presented in Figure 15.

From Figure 15, it can be seen that the SMP from the simulations (35.5 % DSG) is conservatively established compared to the in-service data (45.8 % DSG) demonstrating a cumulative probability of failure smaller than $1E-4$, which means that MSD threat is remote to structural safety and the SMP point from the simulations is well established. This conservatism can also be observed when the SMP is established with the in-service data itself (45.8 % DSG) because the cumulative probabilities of failure are also smaller than $1E-4$. If the SMP point established from the simulations (35.5 % DSG) is checked for MSD initiation behaviour using the in-service distribution presented in Figure 12, it can be seen that approximately 45 % of the fleet would have initiated MSD cracks! Although this probability is high, the cumulative probability of MSD detection from Figure 13 is still small; which means that cracks would not have grown far enough to represent a real threat to the residual strength of the structure. It has to be noted that in case of no detectable MSD cracks at the point of SMP; airworthiness regulators would possibly not recommend repair or structural modifications, but the extension of the point

of SMP (and, consequently, the monitoring period) as a result of further evaluation of the structure. As the SMP given from the simulations fulfils its purpose, the same conclusion applies to the monitoring period since very low cumulative probabilities of MSD failure are involved from the point of ISP to the point of SMP.

4. CONCLUSIONS

1. The MSD model provided good agreement with published experimental work on fatigue of lap splice joints where both crack initiation and propagation stages from the simulations were able to incorporate the experimental data scatter and the mean lives.
2. The spread of the experimental data at both initiation and propagation lives was as large as that of the entire simulations; and this behaviour is also verified from other published work.
3. Evidences from in-service MSD detection strongly indicated that S-N input data obtained from good quality riveted flat lap joint test specimens would not be appropriate for MSD assessment of real aircraft pressurized fuselage panels. Those evidences were also supported by published MSD assessment of a full-scale fatigue test and by a probabilistic fatigue crack initiation analysis using S-N data from good quality riveted lap joints corresponding to the in-service geometrical configuration analysed.
4. The MSD assessment presented was performed with an open hole quality S-N data, and the cumulative probabilities for fatigue crack initiation, crack detection and failure were rationally conservative compared to in-service findings for the corresponding distributions. The differences were in the order of 20%, with the smallest differences belonging to the fatigue crack initiation part of the simulations.
5. In-service data indicated that both the ISP and the SMP were well established from the simulations, and failure due to MSD occurrence was not a threat for structural safety during the monitoring period.

5. FUTURE WORK

For the in-service data comparison discussed in section 3.2, strong evidences were presented indicating that good quality riveted lap joint test specimens were not able to provide S-N input data for MSD assessment of real aircraft fuselage panels. The lack of approach from the literature on such an important issue is surprising. It seems that many authors do believe that, as far as the lap joints are manufactured with the same material and construction techniques employed in the production line, good quality riveted joints can provide S-N data to predict in-service behaviour. What this work showed was that open hole S-N fatigue data demonstrated to be reasonably suitable for MSD analysis of in-service structures. The main question that has to be answered from future workers is whether open hole S-N data is always suitable or not for

different geometrical configurations than the one that has been analysed. It may be that for other fuselage panel configurations, open hole quality S-N data demonstrates inadequacy and, possibly, good quality riveted lap joint S-N data should be more appropriate. This issue has only been started with this work, and further MSD assessments for different in-service aircraft types are needed.

FIGURES

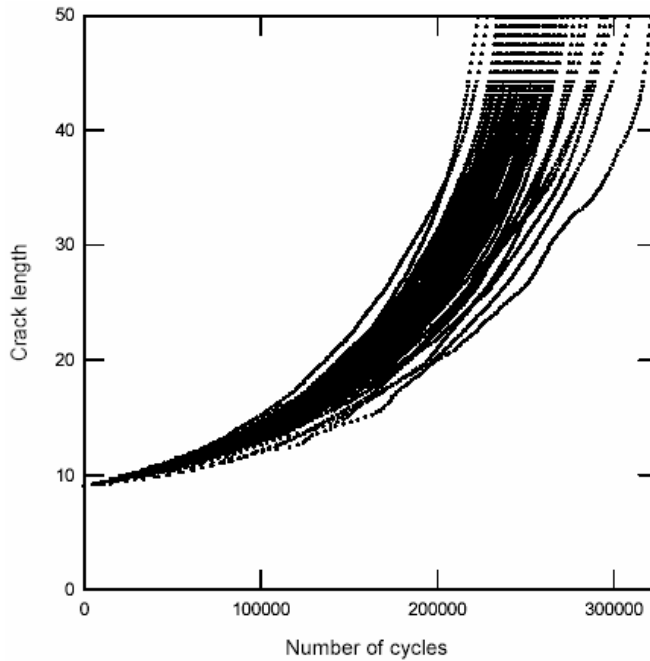


Figure 1: Trajectories of the stochastic crack growth from Virkler [13].

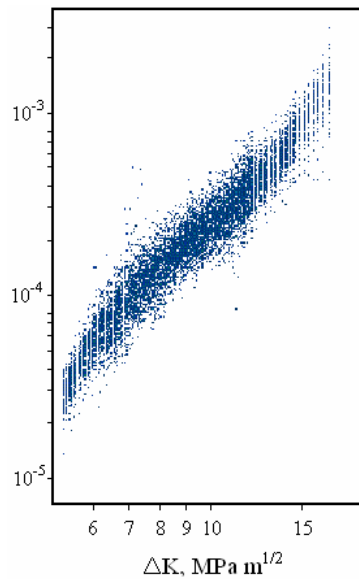


Figure 2: Crack propagation rate dispersion from Virkler [13].

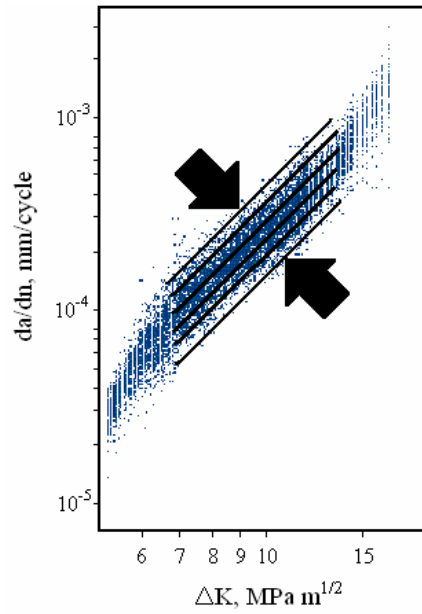


Figure 3: Various crack propagation rate curves for constant 'n' and variable 'C'.

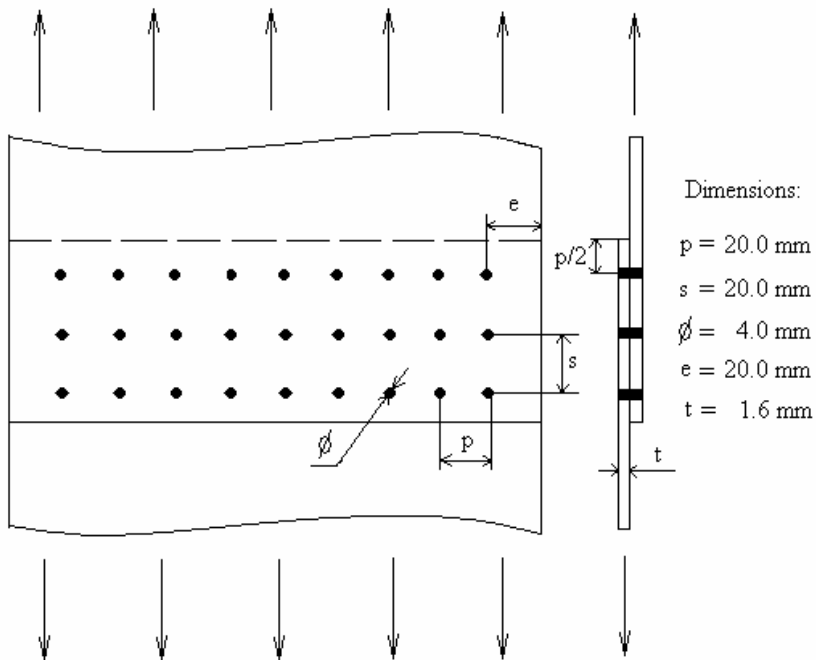


Figure 4: Lap joint configuration.

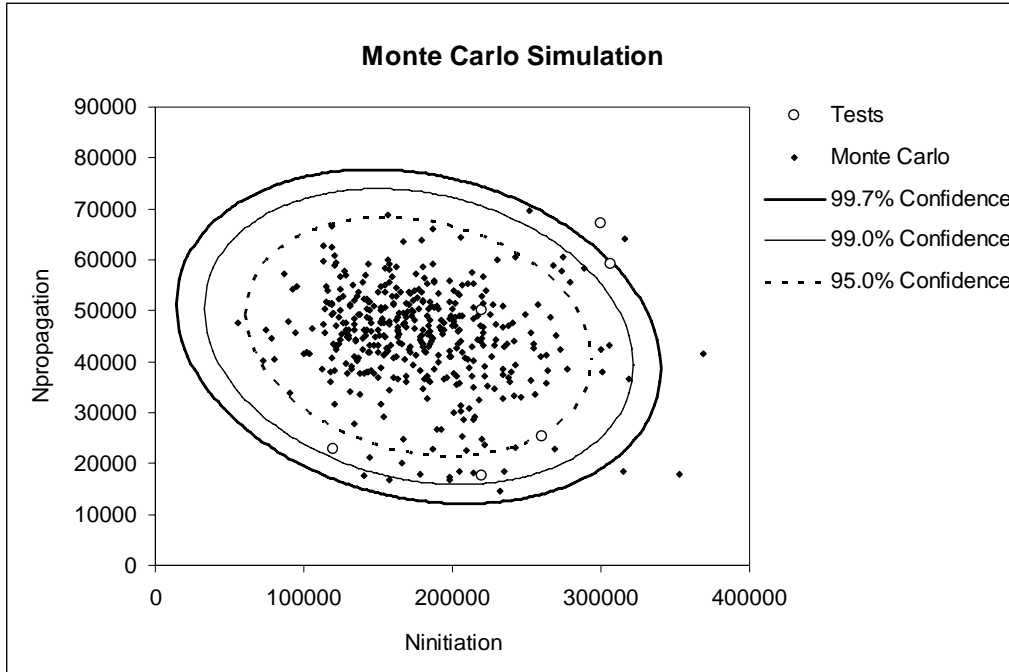


Figure 5: Monte Carlo simulation results and its confidence regions.

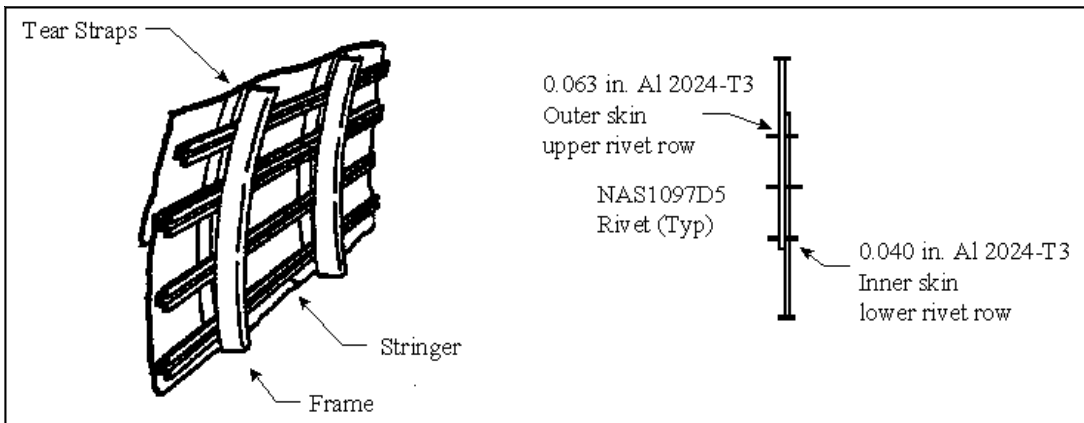


Figure 6: Fuselage lap joint configuration for Boeing 727 aircraft [20].

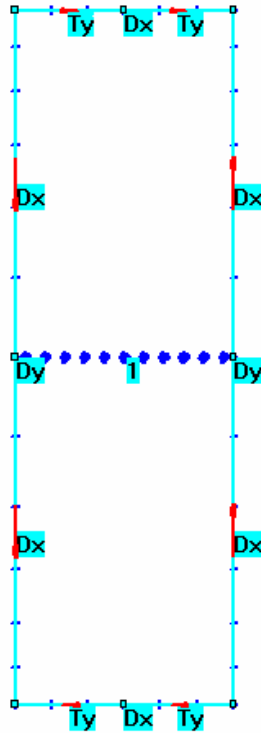


Figure 7: DBE model for the lap joint inner skin lower row from Figure 6.

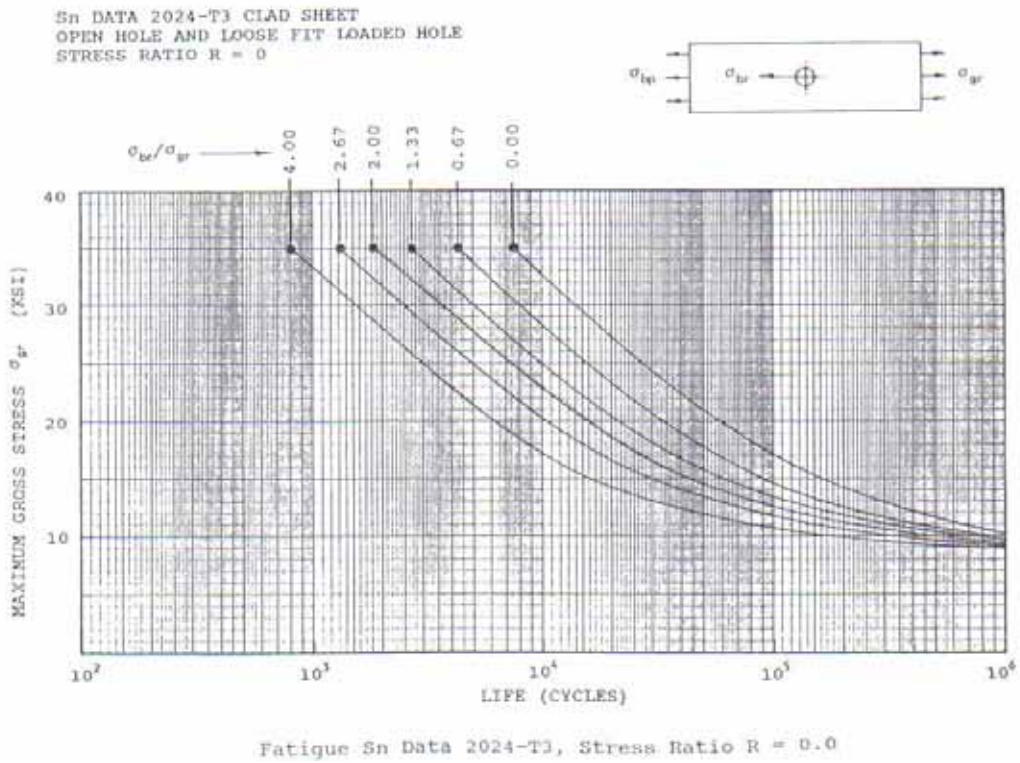


Figure 8: S-N fatigue data for inner skin lower rivet hole from Figure 6 [30].

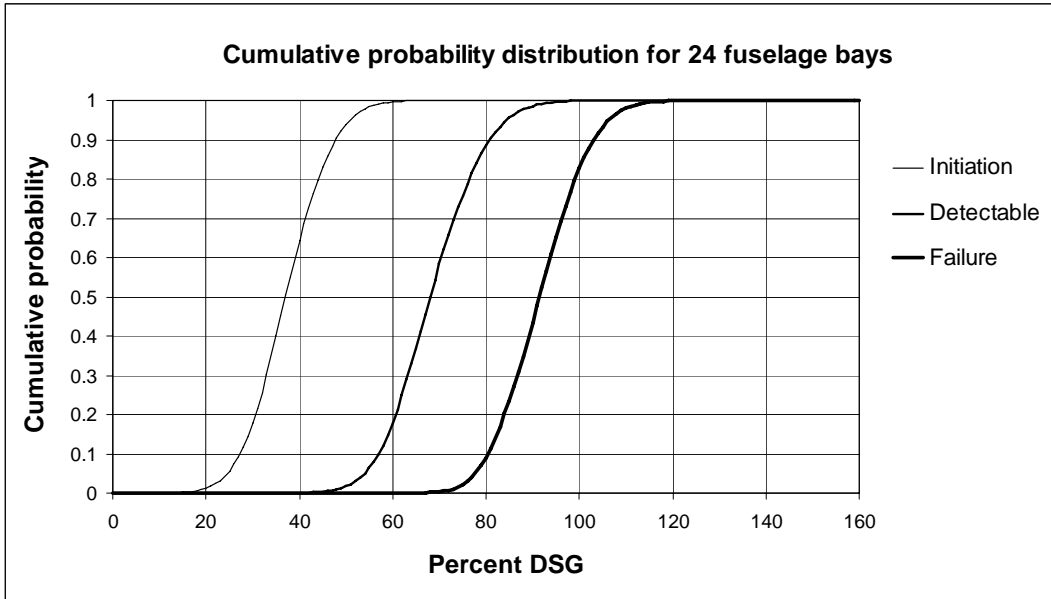


Figure 9: Cumulative probability distributions from teardown inspections [20].

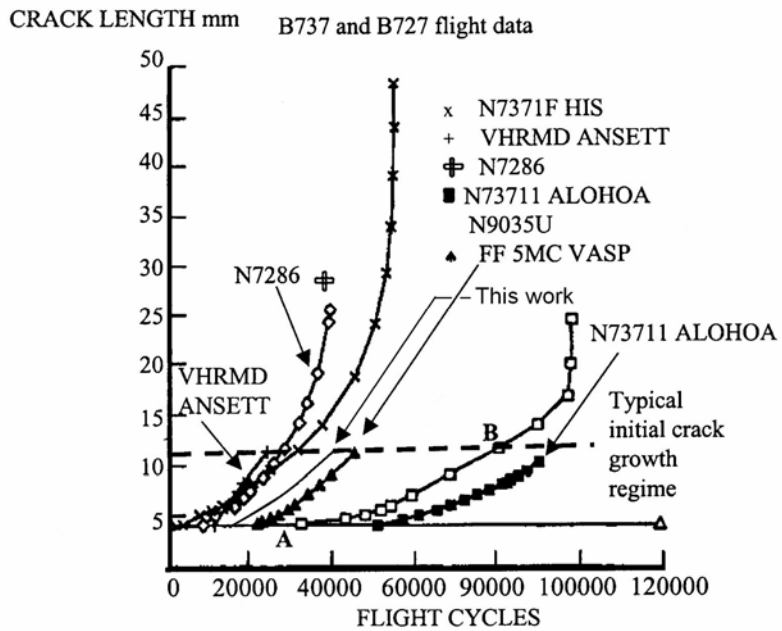


Figure 10: Fleet crack growth data for B-737 and B-727 aircraft [32] comparison to deterministic crack growth from this work.

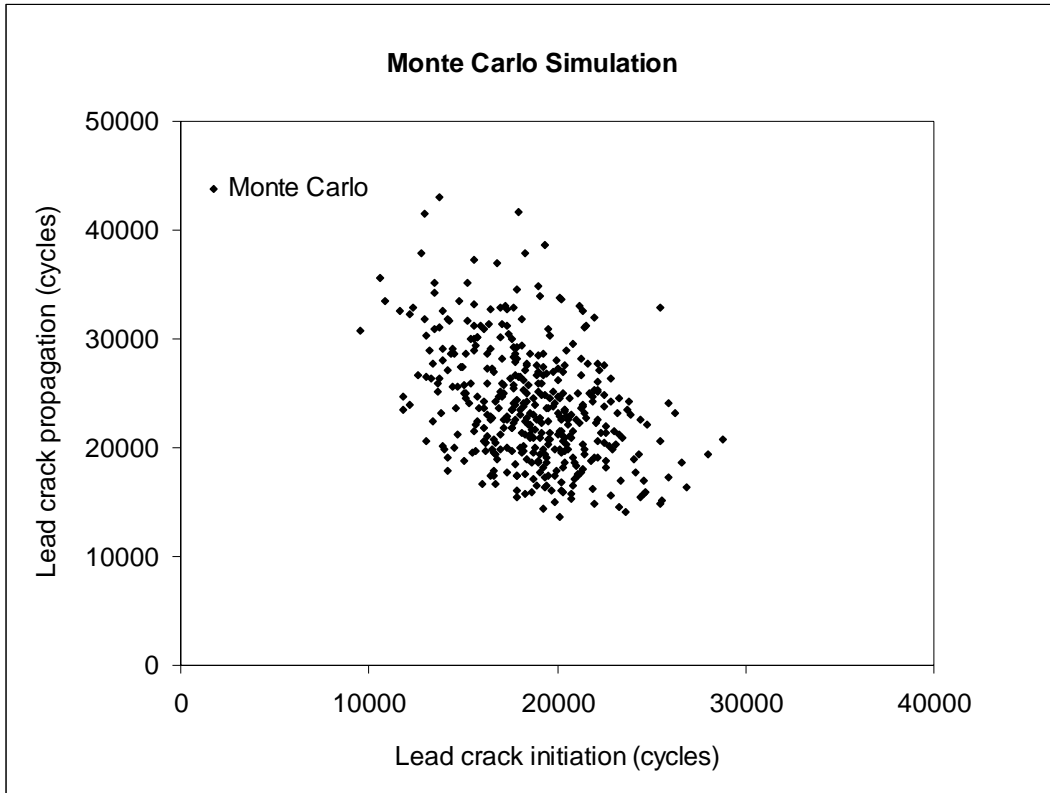


Figure 11: Monte Carlo simulation for teardown inspection comparison.

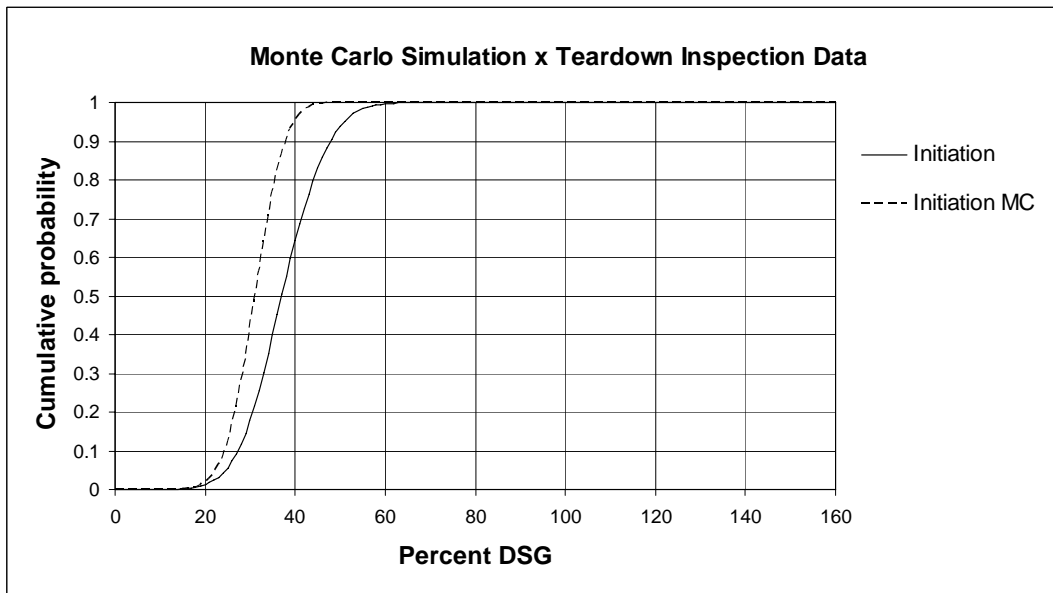


Figure 12: Cumulative probability distribution for initiation of fatigue cracks comparison to teardown inspection data.

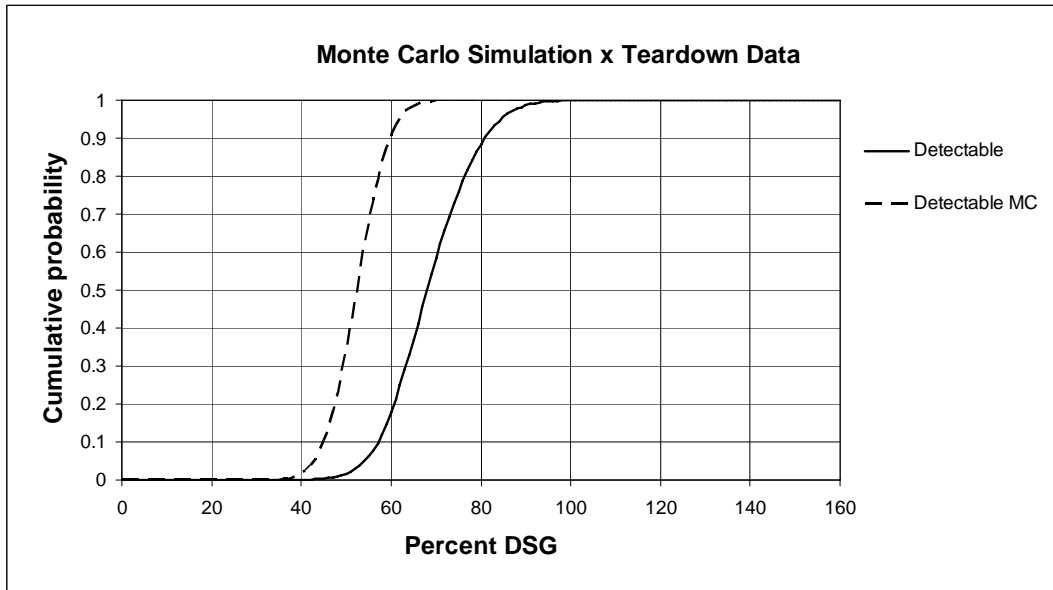


Figure 13: Cumulative probability distribution for detection of fatigue cracks comparison to teardown inspection data.

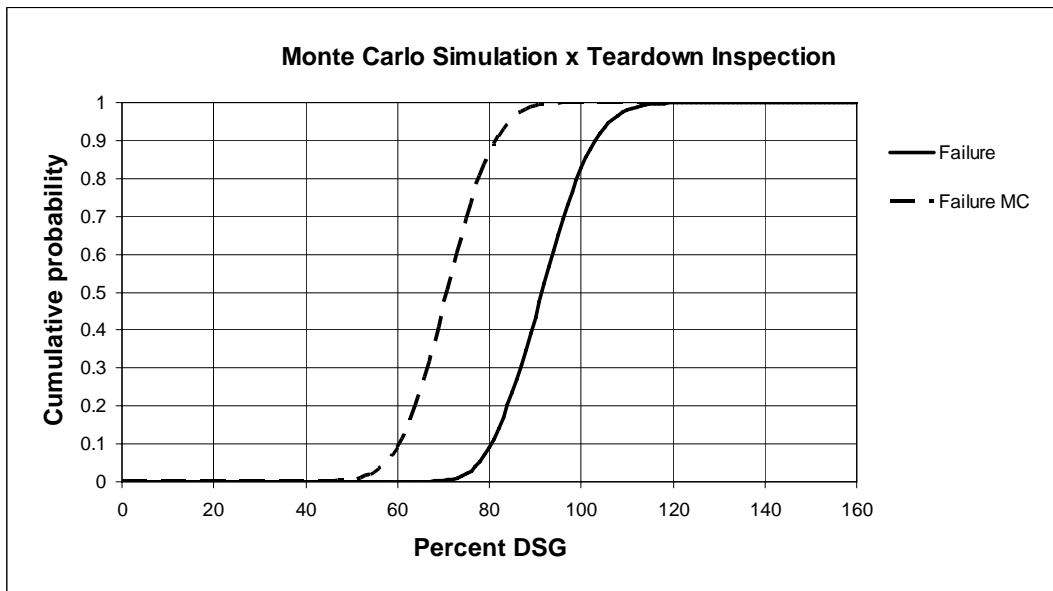


Figure 14: Cumulative probability distribution for failure comparison to teardown inspection data.

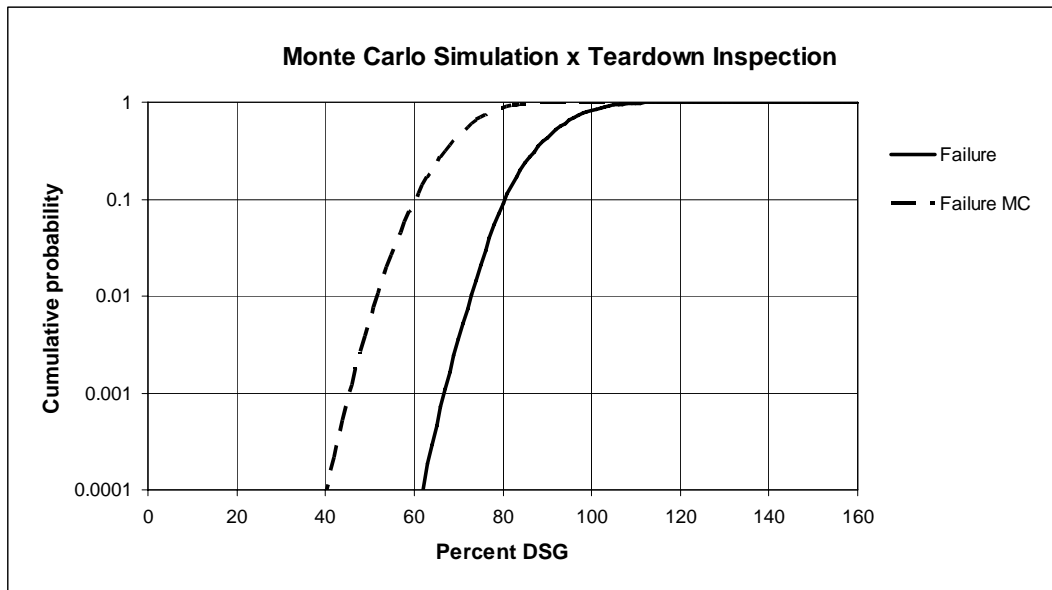


Figure 15: Cumulative probability distribution of failure from Figure 14.

REFERENCES

1. AAWG, Recommendations for Regulatory Action to Prevent Widespread Fatigue Damage in the Commercial Airplane Fleet, a Report of the Airworthiness Assurance Working Group (AAWG) for the Aviation Rulemaking Advisory Committee Transport Aircraft and Engine Issues, March 11, 1999.
2. Santgerma, A., Developpement d'Une Methodologie de Prevision du Comportement des Structures d'Avions Civils en Presence de Dommages Multiples de Fatigue, Doctorate Thesis, Department of Mechanical Engineering, Toulouse, 1997.
3. Proppe, C., Probabilistic Analysis of Multi-Site Damage in Aircraft Fuselages, Computational Mechanics, Vol. 30, pp. 323-329, 2003.
4. Aliabadi, M. H., Rooke, D. P., Numerical Fracture Mechanics, Computational Mechanics Publications, Southampton and Kluwer Academic Publishers, Dordrecht, The Netherlands, 1991.
5. Kebir, A., Roelandt, J. M., Gaudin, J., Monte-Carlo Simulations of Life Expectancy Using the Dual Boundary Element Method, Engineering Fracture Mechanics, Vol. 68, pp. 1371-1384, 2001.
6. ESDU, The Compounding Method of Estimating Stress Intensity Factors for Cracks in Complex Configurations Using Solutions from Simple Configurations, ESDU 78036, 1978.
7. Salgado, N. K., Aliabadi, M.H., Boundary Element Analysis of Fatigue Crack Propagation in Stiffened Panels, Journal of Aircraft, Vol. 35, No. 1, pp. 122-130, 1998.
8. Salgado, N. K., Aliabadi, M. H., The Analysis of Mechanically Fastened Repairs and Lap Joints, Fatigue Fract. Engng. Struct., Vol. 20, No. 4, pp. 583-593, 1997.
9. Salgado, N. K., Damage Tolerance Design System DTD, Version 5.0, Empresa Brasileira de Aeronautica, S. J. Campos – S. P., Brazil, 1999.
10. Tanaka, K., Fatigue Crack Propagation from a Crack Inclined to the Cyclic Tensile Axis, Engineering Fracture Mechanics, Vol. 6, pp. 493-507, 1974.
11. Swift, T., Damage Tolerance Capacity, in: Fatigue of Aircraft Materials-Proceedings of the Specialists' Conference, Dedicated to the 65th Birthday of J. Schijve, Delft University Press, pp. 351-387, 1992.

12. USAF, Airplane Damage Tolerance Requirements, Military Specification, MIL-A-83444, 1974.
13. Virkler, D. A., Hillberry, B. M., Goal, P. K., Journal of Engineering Materials and Technology, Vol. 101, pp. 148-153, 1979.
14. Xing, J. and Hong, Y. J., A Maximum Likelihood Method for Estimates of the Statistics of the Crack Growth Behaviour, International Journal of Pressure Vessels and Piping 76: 641-646, 1999.
15. Cavallini, G., Galatolo, R., Cattaneo, G., An experimental and numerical analysis of multi-site damaged butt-joints, Proceedings of the 20th ICAF Symposium, Vol. 1, Bellevue, Washington, U.S.A., July 1999.
16. Ostergaard, D. F., Hillberry, B. M., Characterization of the variability in fatigue crack propagation data, Probabilistic Fracture Mechanics and Fatigue Methods: Application for Structural Design and Maintenance, STM STP 798, 1983.
17. Foulquier, J., Fatigue Tests on Simple Lap Joint Specimens, Report SMAAC TR-3.2-04-1.3/AS, 1997.
18. Press, W. H., Teukolsky, S. A., Vetterling, W. T., Flannery, B. P., Numerical Recipes in C – The Art of Scientific Computing, Cambridge University Press, Second Edition, 1992.
19. Arnold, B., Shavelle, R. M., Joint Confidence Sets for the Mean and Variance of a Normal Distribution, The American Statistician, Vol. 52, No. 2, 1998.
20. Steadman, D., Carter, A., Ramakrishnan, R., Characterization of MSD in an in-service fuselage lap joint, 3rd Joint FAA/DoD/NASA Conference on Aging Aircraft, Albuquerque, New Mexico, September 1999.
21. Schmidt, H.-J., Schimidt-Brandecker, B., Trey, H., AIRBUS A300 fuselage program for life extension and widespread fatigue damage evaluation, The 3rd Joint FAA/DoD/NASA Conference on Aging Aircraft, Albuquerque, New Mexico, USA, September 1999.
22. Garcia, A. N., Irving, P. E., MSD simulation in lap joints using a DBEM model, 24th International Congress of the Aeronautical Sciences (ICAS 2004) Yokohama, Japan, 29 August – 3 September, 2004.
23. Okada T., Terada H., Dybskiy P., Fatigue behaviour of lap joint of fuselage model structure. Fifth Joint NASA/FAA/DoD Conference on Aging Aircraft, Orlando, Florida, 2001.
24. Wanhill, R. J. H., Koolloos, M. F. J., Fatigue and corrosion in aircraft pressure lap splices, International Journal of Fatigue, No. 23, pp. S337-S347, 2001.
25. Bakuckas, J. G., Carter, A., Destructive evaluation and extended fatigue testing of retired aircraft fuselage structure, 11th International Conference on Fracture (ICF 11), Turin, Italy, March 20-25, 2005.
26. Garcia, A. N., Multiple Site Damage of Aeronautical Riveted Joints, Ph.D. Thesis, Cranfield University, Cranfield, U.K., September 2005.
27. Bellinger, N. C., Forsyth, D. S., Komorowski, J. P., Damage characterization of corroded 2024-T3 fuselage lap joints, 5th Joint NASA/FAA/DoD Conference on Aging Aircraft, Orlando, Florida, September, 2001.
28. Liao, M., Bellinger, N., Komorowski, J. P., Analytical methodologies for fatigue life prediction of corroded fuselage splices, 5th Joint NASA/FAA/DoD Conference on Aging Aircraft, Orlando, Florida, September, 2001.
29. Horst, P., Schmidt, H., A concept for evaluation of MSD based on probabilistic assumptions, AGARD Conference Proceedings 568, Neuilly-Sur-Seine, France, 1995.
30. Swift, T., Repairs to damage tolerant aircraft, Atluri, S. N., Sampath, S. G., Tong, P., eds., Structural Integrity of Aging Airplanes, Springer-Verlag Berlin, Heidelberg, 1991.
31. Nesterenko, G. I., Basov, V. N., Fatigue strength of al-alloys in case of random spectra loading, 24th International Congress of the Aeronautical Sciences (ICAS 2004) Yokohama, Japan, 29 August – 3 September, 2004.
32. Jones, R., Peng, D., A simple method for computing the stress intensity factors for cracks at notches, Engineering Failure Analysis, no. 9, pp. 683-702, 2002.